



Journal of Coordination Chemistry

Publication details, including instructions for authors and subscription information:

<http://www.tandfonline.com/loi/gcoo20>

The supramolecular assembly of tetraaqua-(pyridine-2,5-dicarboxylato)-copper(II) complex: crystal structure, TD-DFT approach, electronic spectra, and photoluminescence study

Soumen Manna^a, Soumen Mistri^a, Ennio Zangrando^b & Subal Chandra Manna^a

^a Department of Chemistry and Chemical Technology, Vidyasagar University, Midnapore, India

^b Department of Chemical and Pharmaceutical Sciences, University of Trieste, Trieste, Italy

Accepted author version posted online: 27 Mar 2014. Published online: 23 Apr 2014.



[Click for updates](#)

To cite this article: Soumen Manna, Soumen Mistri, Ennio Zangrando & Subal Chandra Manna (2014) The supramolecular assembly of tetraaqua-(pyridine-2,5-dicarboxylato)-copper(II) complex: crystal structure, TD-DFT approach, electronic spectra, and photoluminescence study, *Journal of Coordination Chemistry*, 67:7, 1174-1185, DOI: [10.1080/00958972.2014.909035](https://doi.org/10.1080/00958972.2014.909035)

To link to this article: <http://dx.doi.org/10.1080/00958972.2014.909035>

PLEASE SCROLL DOWN FOR ARTICLE

Taylor & Francis makes every effort to ensure the accuracy of all the information (the "Content") contained in the publications on our platform. However, Taylor & Francis, our agents, and our licensors make no representations or warranties whatsoever as to the accuracy, completeness, or suitability for any purpose of the Content. Any opinions and views expressed in this publication are the opinions and views of the authors, and are not the views of or endorsed by Taylor & Francis. The accuracy of the Content should not be relied upon and should be independently verified with primary sources of information. Taylor and Francis shall not be liable for any losses, actions, claims, proceedings, demands, costs, expenses, damages, and other liabilities whatsoever or howsoever caused arising directly or indirectly in connection with, in relation to or arising out of the use of the Content.

This article may be used for research, teaching, and private study purposes. Any substantial or systematic reproduction, redistribution, reselling, loan, sub-licensing, systematic supply, or distribution in any form to anyone is expressly forbidden. Terms & Conditions of access and use can be found at <http://www.tandfonline.com/page/terms-and-conditions>

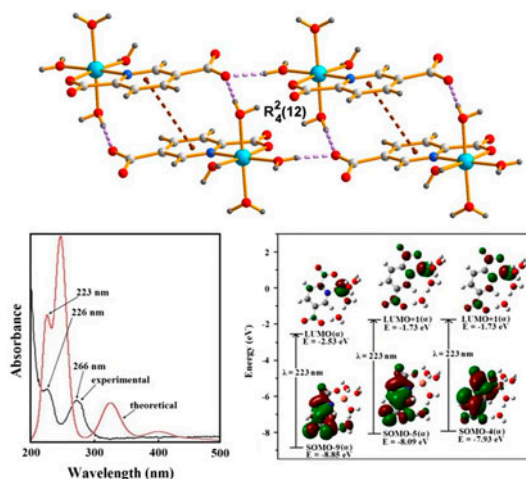
The supramolecular assembly of tetraaqua-(pyridine-2,5-dicarboxylato)-copper(II) complex: crystal structure, TD-DFT approach, electronic spectra, and photoluminescence study

SOUMEN MANNA[†], SOUMEN MISTRI[†], ENNIO ZANGRANDO[‡] and
SUBAL CHANDRA MANNA^{*†}

[†]Department of Chemistry and Chemical Technology, Vidyasagar University, Midnapore, India

[‡]Department of Chemical and Pharmaceutical Sciences, University of Trieste, Trieste, Italy

(Received 24 August 2013; accepted 28 February 2014)



The copper(II) complex, $\{[\text{Cu}(2,5\text{-pdc})(\text{H}_2\text{O})_4] \cdot \text{H}_2\text{O}\}$ (**1**) [2,5-pdc = pyridine-2,5-dicarboxylate], has been synthesized and characterized by elemental analysis, IR spectroscopy, and X-ray crystallography. The metal shows a distorted octahedral coordination sphere and in solid state the complex forms a 3-D supramolecular network via hydrogen bonding and off-center anti-parallel π - π stacking interactions between py rings. At room temperature, **1** exhibits fluorescence in methanolic solution [$\lambda_{\text{ex}} = 226$ nm, $\lambda_{\text{em}} = 309$, 330, and 341 nm]. The geometry optimization at the B3LYP/LanL2DZ level led to a five-coordinate copper having a distorted square pyramidal geometry. The electronic spectrum of this compound is compared with the results obtained by employing density functional theory (DFT) and time dependent density functional theory calculations.

Keywords: Copper complex; Pyridine-2,5-dicarboxylate; Supramolecular assembly; DFT analysis

*Corresponding author. Email: scmanna@mail.vidyasagar.ac.in

1. Introduction

One of the important goals of crystal engineering is targeted at the expected assembly of molecular species into extended architectures [1]. Inorganic crystal engineering [2] is focused on the functionalization of material in the solid state and the properties of compounds depend on the entire crystalline aggregate that is controlled by weak interactions. Therefore, one of the purpose of research in this field is the development of supramolecular self-assembly controlled by covalent or non-covalent interactions, which can lead to materials with a variety of potential applications such as mesoporous material [3] and molecular/optoelectronic devices [4]. Among weak non-covalent interactions, hydrogen bonds are commonly used as “structure directing” and hence allow speculating on application in crystal design [5]. Thus, considerable interest is devoted to the synthesis of supramolecular assemblies employing various types of hydrogen bonds, such as O–H···O, N–H···O, N–H···N, N–H···S, and C–H···O [6], beside coordination bonds between metal ion and ligands [7]. In addition stacking between aromatic rings plays an important role for tuning the crystal structure topology [8]. In fact intermolecular attraction energy through parallel face-to-face (also off-center arrangement of aromatic rings) and edge-to-face (T-shaped arrangement of aromatic planes) orientations contributes up to 10 kJ/M [9].

Carboxylate groups, acting in a variety of coordination modes, have been extensively applied in the synthesis of complexes with the aim to form large, tightly bound metal cluster aggregates, often with specific and directional hydrogen bonds to modulate the molecular architecture [10]. Over the last few years we have been actively engaging in the synthesis of metal-carboxylate coordination networks [10(a), 10(g), 11].

The pyridine 2,5-dicarboxylate dianion (2,5-pdc) with a 180° angle between the carboxylate groups has been used as an efficient coordinating agent (chart 1) in designing inorganic supramolecular systems for its versatile coordination modes as well as for its hydrogen bonding capability [12]. During the course of our investigations of supramolecular assemblies by using pyridinyl carboxylates, we have isolated a copper(II) compound, {[Cu(2,5-pdc)(H₂O)₄]·H₂O} (**1**) [2,5-pdc = pyridine-2,5-dicarboxylate], possessing a 3-D network structure realized by hydrogen bonding and off-center anti-parallel interactions of py rings [9(d)]. A study of the electronic spectra and time-dependent density functional theory (TD-DFT) calculations shows that electronic spectral transitions of **1** at 226 and 266 nm correspond to intra-ligand charge transfer transitions of the coordinated 2,5-pdc ligand.

2. Materials and methods

High-purity pyridine-2,5-dicarboxylic acid (Aldrich) was purchased and used as received. All other chemicals were of analytical grade. Solvents used for spectroscopic studies were purified and dried by standard procedures before use [13].

Elemental analyses (carbon, hydrogen, and nitrogen) were performed using a Perkin-Elmer 240C elemental analyzer. IR spectra were recorded as KBr pellets on a Bruker Vector 22FT IR spectrophotometer operating from 400 to 4000 cm⁻¹. Electronic absorption spectra were obtained with a Shimadzu UV-1601 UV–vis spectrophotometer at room temperature. Quartz cuvettes with a 1 cm path length and a 3 cm³ volume were used for all measurements. Emission spectra were recorded on a Hitachi F-7000 spectrofluorimeter. Room temperature (300 K) spectra were obtained in methanolic solution using a quartz cell of 1 cm path length. The slit width was 2.5 nm for both excitation and emission.

2.1. Synthesis of $[Cu(2,5-pdc)(H_2O)_4] \cdot H_2O$ (**1**)

A methanolic solution (10 mL) of pyridine-2,5 dicarboxylic acid (1 mM, 0.167 g) was allowed to react with a methanolic solution (10 mL) of $Cu(ClO_4)_2 \cdot 6H_2O$ (1 mM, 0.370 g) and stirred for 5 min. Then, a methanolic solution (5 mL) of triethylamine (2 mM) was slowly poured with stirring. The whole green-colored reaction mixture was stirred for 2 h and filtered. The filtrate was kept in a $CaCl_2$ desiccator and green single crystals suitable for X-ray determination were obtained after a few days. Yield: 0.254 g (80%). Anal. Calcd for $C_7H_{13}CuNO_9$ (%): C, 26.35; H, 3.45; N, 4.39%. Found: C, 26.33; H, 3.41; N, 4.42. The infrared spectra exhibited the following absorptions: 3000–3500 (br), 2974 (w), 1628 (s), 1560 (vs), 1470 (s), 1412 (s), 837 (w), and 538 (vw) cm^{-1} .

2.2. Single-crystal X-ray diffraction

The X-ray data collection for **1** was carried out at 293(2) K with $MoK\alpha$ radiation ($\lambda = 0.71073 \text{ \AA}$) on a Bruker Smart Apex diffractometer equipped with CCD. Cell refinement, indexing, and scaling of the data-sets were done by using programs Bruker Smart Apex and Bruker Saint packages [14]. The data were corrected for absorption with SADABS program [15]. The structure was solved by direct methods and subsequent Fourier analyses [16] and refined by the full-matrix least squares method based on F^2 with all observed reflections [16]. Hydrogens of water molecule, first detected in the Δ Fourier map, were refined with constraints on O–H distances (0.85 \AA). Graphical programs used are those included in the WinGX System, Ver 1.80.05 [17] and Diamond [18]. Crystal data and details of refinements are given in table 1.

Table 1. Crystal data and details of refinements of **1**.

| | |
|---|-------------------|
| Empirical formula | $C_7H_{13}CuNO_9$ |
| Formula weight | 318.72 |
| Temperature (K) | 293 |
| Crystal system | Triclinic |
| Space group | $P\bar{1}$ |
| a (\AA) | 6.756(6) |
| b (\AA) | 8.436(5) |
| c (\AA) | 10.801(5) |
| α ($^\circ$) | 84.66(9) |
| β ($^\circ$) | 83.16(8) |
| γ ($^\circ$) | 67.79(7) |
| V (\AA^3) | 565.1(7) |
| Z | 2 |
| D_c ($g\ cm^{-3}$) | 1.873 |
| μ $MoK\alpha/mm^{-1}$ | 1.98 |
| $F(000)$ | 326 |
| θ_{range} ($^\circ$) | 1.9–25.4 |
| Reflections collected | 8582 |
| Unique reflections | 2054 |
| R_{int} | 0.064 |
| Observed [$I > 2\sigma(I)$] | 1615 |
| Parameters | 175 |
| Goodness of fit (F^2) | 1.052 |
| $R1, wR2$ [$I > 2\sigma(I)$] ^a | 0.0580, 0.1601 |
| $\Delta\rho/e\ \text{\AA}^{-3}$ | 1.734, -0.608 |

^a $R1 = \sum ||F_o| - |F_c|| / \sum |F_o|$, $wR2 = [\sum w(F_o^2 - F_c^2)^2] / \sum w(F_o^2)^2$.

2.3. Theory and computational methods

All computations were performed using the Gaussian 09 (G09) software package, [19] by using the Becke's three-parameter hybrid exchange functional and the Lee–Yang–Parr non-local correlation functional (B3LYP) [20]. In the calculation, the 6-31G (d-p) basis set was assigned to all elements with the exception of copper, for which the Los Alamos effective core potentials plus the Double Zeta (LanL2DZ) [21] basis set were employed. The geometric structure of the complex in the ground state (doublet) was fully optimized at the B3LYP level. The Vibration frequency calculations were performed to insure that the optimized geometries represent local minima associated with positive eigen values only.

Vertical electronic excitations based on B3LYP were obtained with the TD-DFT formalism [22] in methanol using the conductor-like polarizable continuum model (CPCM) [23]. GaussSum [24] was used to calculate the fractional contribution of various groups to each molecular orbital. Calculated coordination geometries of methanol-solvated complex and the data in gas phase using LanL2DZ basis set are reported in table 2.

3. Results and discussion

3.1. IR, electronic spectral studies, and photoluminescence properties

The most important absorption bands in IR spectroscopy of **1** are summarized in the experimental section and tabulated in table 1S, see online supplemental material at <http://dx.doi.org/10.1080/00958972.2014.909035>. The spectrum of **1** exhibits bands at 1628 and 1412 cm^{-1} , corresponding to $\nu_{\text{as}}(\text{OCO})$ and $\nu_{\text{s}}(\text{OCO})$, respectively. Aromatic $\nu(\text{C}=\text{C}, \text{C}=\text{N})$

Table 2. Experimental and calculated [†] coordination bond lengths (Å) and angles (°) for **1**.

| Bond lengths | X-ray data | Calculated [†] | |
|--------------|------------|-------------------------------------|---------------------------------|
| | | CPCM in methanol: basis set LanL2DZ | In gas phase: basis set LanL2DZ |
| Cu–O1 | 2.052(4) | 1.979 | 1.963 |
| Cu–O5 | 2.105(4) | 2.256 | 3.379 |
| Cu–O6 | 2.035(4) | 2.019 | 2.136 |
| Cu–O7 | 2.085(4) | 1.991 | 1.976 |
| Cu–O8 | 2.061(4) | 4.113 | 3.436 |
| Cu–N1 | 2.072(4) | 1.986 | 2.009 |
| O1–Cu–O6 | 92.32(17) | 94.08 | 90.64 |
| O1–Cu–O7 | 173.18(14) | 161.92 | 165.05 |
| O1–Cu–O8 | 91.07(17) | – | – |
| O1–Cu–N1 | 79.46(16) | 81.92 | 82.57 |
| O6–Cu–O7 | 94.12(17) | 87.84 | 90.13 |
| O6–Cu–O8 | 87.78(18) | – | – |
| O6–Cu–N1 | 171.74(16) | 173.61 | 164.09 |
| O7–Cu–O8 | 86.96(17) | – | – |
| O7–Cu–N1 | 94.12(17) | 94.42 | 100.12 |
| O8–Cu–N1 | 93.12(18) | – | – |
| O5–Cu–O1 | 93.19(17) | 100.54 | 45.82 |
| O5–Cu–O6 | 87.80(19) | 78.07 | 45.40 |
| O5–Cu–O7 | 89.29(17) | 97.44 | 131.05 |
| O5–Cu–O8 | 173.99(15) | – | – |
| O5–Cu–N1 | 91.84(18) | 107.48 | 128.07 |

[†]CPCM = Conductor-like polarizable continuum model.

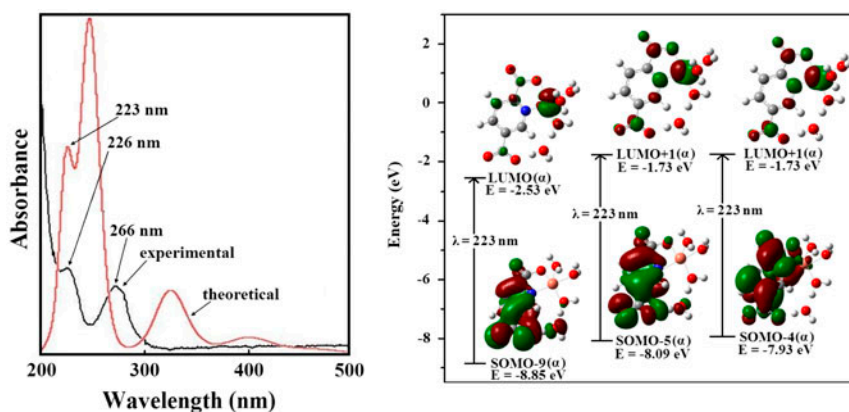


Figure 1. Theoretical (red line) and experimental (black line) electronic spectra (left) of **1**. The most prominent MOs involving transitions (right) and their diagrams (see <http://dx.doi.org/10.1080/00958972.2014.909035> for color version).

stretching vibrations appear in the region at $1470\text{--}1560\text{ cm}^{-1}$. The band at 2974 cm^{-1} corresponds to the aromatic $\nu(\text{C-H})$ stretching vibrations. A strong broad band in the region $3000\text{--}3500\text{ cm}^{-1}$ is due to the $\nu(\text{O-H})$ stretching vibration of water molecules [25]. The IR spectrum of **1** also shows the band corresponding to $\rho_r(\text{H}_2\text{O})$ (at 837 cm^{-1}) and to $\rho_w(\text{H}_2\text{O})$ (at 538 cm^{-1}) indicating the presence of coordinated water molecules. Theoretically possible IR spectral bands of optimized structures (using LanL2DZ as basis set in gas phase, and using CPCM model in methanol), listed in table 1S, are in good agreement with the experimental results.

The electronic spectrum of **1** (figure 1), recorded in methanol, shows significant transitions at 226 nm ($\epsilon \sim 3.52 \times 10^2\text{ L M}^{-1}\text{ cm}^{-1}$) and 266 nm ($\epsilon \sim 2.68 \times 10^2\text{ L M}^{-1}\text{ cm}^{-1}$) assigned to intra-ligand charge transfer of the coordinated 2,5-pdc ligand.

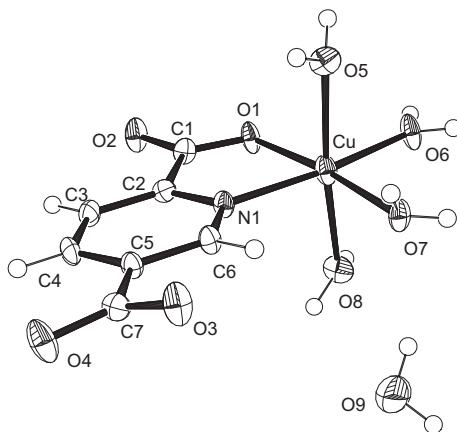


Figure 2. ORTEP diagram (ellipsoids at 50% probability) of **1**.

On excitation at 226 nm, **1** exhibits luminescence bands at 309, 330, and 341 nm in methanol at room temperature (figure 1S). These band positions remain unchanged when λ_{ex} is varied between 216 and 236 nm.

3.2. Description of crystal structure

Complex $[\text{Cu}(2,5\text{-pdc})(\text{H}_2\text{O})_4]\cdot\text{H}_2\text{O}$ (**1**) crystallizes in the triclinic space group $P\bar{1}$ and an ORTEP view of the asymmetric unit is shown in figure 2. In the discrete complex the copper ion is chelated by the pyridyl nitrogen and a carboxylato oxygen of 2,5-pdc and bound to four water molecules in a slightly distorted octahedral geometry. The Cu–O bond lengths vary in the range 2.035(4)–2.105(4) Å and the Cu–N bond distance is 2.072(4) Å. The coordination bond angles of *cis* located donors show values in the range 86.96(17)°–94.12(17)°, while the chelating N1–Cu–O1 angle is 79.46(16)° (table 2). The packing view down the *b*-axis reveals that adjacent copper complexes are alternately arranged to form a supramolecular 1-D chain via off-center anti-parallel π – π stacking interactions (centroid-to-centroid distance 3.805(5) Å, slippage of 1.818 Å table 2S) and connected by pairwise coupling of O–H \cdots O interactions. Although the term π – π interactions is widely overused in the literature, the antiparallel-displaced geometry for py rings was shown to be the most stable interaction between these heterocycle rings [9(d)]. Hydrogen bond interactions form a $R_4^2(12)$ supramolecular synthon [26] (figure 3) giving rise to a 2-D layer parallel to the *ac* plane. The O(donor)–O(acceptor) distances are in the range 2.704(6)–2.719(5) Å (table 4S). These 1-D chains are again involved in H-bonding interactions with the lattice water molecule O(9) to form a 3-D supramolecular architecture. The formation of the 3-D supramolecular network evidences also the formation of $R_6^4(24)$ synthons (figure 4). A C=O(4) $\cdots\pi$ distance of 3.775(6) Å was measured in the structure, but being the carbonyl almost parallel to the 2,5-pdc face (7.29°, table 3S), the interaction should be rather weak or even repulsive [27].

The pyridine-2,5-dicarboxylic acid represents a versatile molecule to be used as ligand for the construction of coordination polymers, but here the presence of coordinated aqua ligands at the copper center led to a discrete complex and hampered the participation of a second 2,5-pdc carboxylate in coordination. In fact a reduced number or lack of water molecules led to 1-D polymers $[\text{Cu}(2,5\text{-pdcH}_2)]$ [28], 2-D coordination networks $([\text{Cu}(2,5\text{-pdc})(\text{H}_2\text{O})])$ [29] and $[\text{Cu}_2(2,5\text{-pdc})_2(\text{H}_2\text{O})_2]\cdot 4\text{H}_2\text{O}$ [30, 31], and 3-D in the

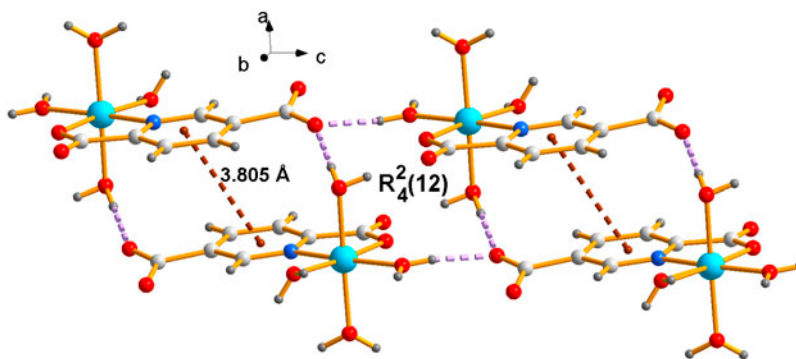


Figure 3. π – π interactions and $R_4^2(12)$ H-bonded synthon in **1** giving a 2-D supramolecular layer.

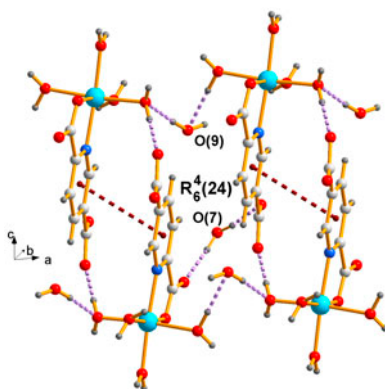


Figure 4. The $R_6^4(24)$ hydrogen bonded synthon formed in **1** with lattice water O(9).

Table 3. Structure of copper-(2,5-pdc) complexes with ligand coordination mode.

| Compound | Structure | 2,5-pdc coordination mode (see chart 1) | Ref. |
|---|--|--|-----------|
| [Cu(2,5-pdc)(H ₂ O) ₄ ·H ₂ O] | Mononuclear complex, 3-D supramolecular structure through H-bonding and π - π stacking | η^2 (NO) | This work |
| [Cu(2,5-pdcH ₂) ₂] | 1-D coordination polymer with Cu-O contacts of 2.70 Å | μ - η^3 (<i>cis</i> -NO,O') | [27] |
| [Cu(2,5-pdc)(H ₂ O)] | 2-D coordination polymer with Cu-O bonds of 2.57 Å, 3-D supramolecular structure through H-bonding | μ - η^3 (<i>trans</i> -NO,O') | [28] |
| [Cu ₂ (2,5-pdc)(H ₂ O)]·2H ₂ O | 2-D coordination polymer with Cu-O bonds of 2.63 Å | μ^5 - η^2 : η : η : η (NO, O,O',O'') | [29, 30] |
| [Cu ₃ (2,5-pdc) ₃ (H ₂ O) ₃ ·6H ₂ O] | 3-D coordination polymer with Cu-O bonds of 2.67 Å | μ^5 - η^2 : η : η : η (NO,O, O',O'') | [30] |

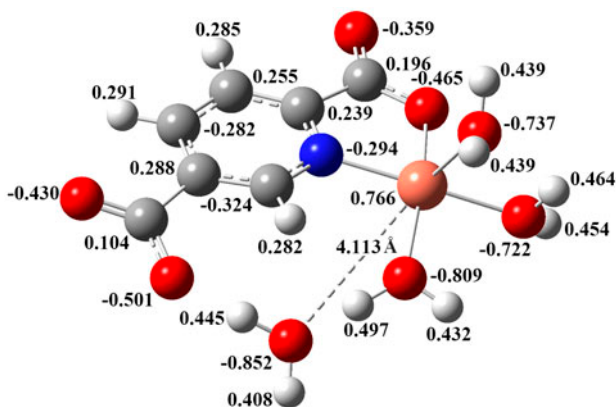


Figure 5. Optimized geometry of **1** (using CPCM model in methanol) with Mulliken charge distribution.

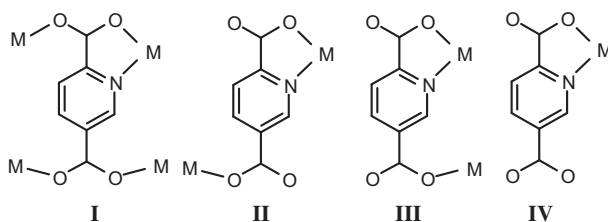


Chart 1. Hapticity of pdc: $\mu_5\text{-}\eta_2\text{:}\eta\text{:}\eta\text{:}\eta$, (NO,O,O',O') (I); $\mu\text{-}\eta_3$, *trans*-(NO,O') (II); $\mu\text{-}\eta_3$, *cis*-(NO,O') (III) and chelating η_2 , (NO) (IV).

polymorph of formula $[\text{Cu}_3(2,5\text{-pdc})_3(\text{H}_2\text{O})_3]\cdot 6\text{H}_2\text{O}$ [31]. The solid-state structures are governed by long $\text{Cu}\cdots\text{O}$ contacts (Jahn–Teller distorted arrangement), which emphasize the tendency of solvothermal synthesis to generate extended lattices if possible. Details of the mentioned structures are summarized in table 3.

3.3. DFT calculations

Since the coordinated water molecules can markedly affect the hydrogen bonding of the structure [32], DFT and TD-DFT computations were performed on the $[\text{Cu}(2,5\text{-pdc})(\text{H}_2\text{O})_4]$ (1A) complex (thus excluding lattice water molecules) to establish its electronic structure and spectral transitions. The geometric structure of the isolated 1A was fully optimized at the Becke's three-parameter hybrid exchange functional and the Lee–Yang–Parr non-local correlation functional (B3LYP) level in the ground state (doublet). The optimized structure of 1A along with Mulliken charge distribution is depicted in figures 5 and 2S, and calculated bond lengths and angles along with the experimentally measured values are listed in table 2. It is interesting to note that calculations led to an optimized structure where the copper(II) center is five-coordinate with only three aqua ligands. Calculated (using CPCM model in methanol, LanL2Dz basis set) distance of Cu(II) atom from the split (fourth) water molecule is 4.143 Å, indicating no coordination interaction between the metal and this water molecule. The trigonality τ_5 parameter [33] for five-coordinate complexes allows evaluation of deviations between regular trigonal bipyramidal and square pyramidal geometry, calculated as $(\alpha - \beta)/60$, where α and β are the two largest coordination bond angles. Hence, a regular trigonal bipyramidal structure with D_{3h} symmetry has $\tau = 1$ and a regular C_{4v} square pyramidal geometry has $\tau = 0$. From the theoretical data of 1A, τ is calculated 0.19, indicating for the copper center a distorted square pyramidal coordination sphere (SPY-5). The calculated structure in the gas phase shows a four-coordinate copper(II) centre with two water molecules left aside. Calculated (in gas phase, LanL2Dz basis set) distances of Cu(II) atom from these water molecules are 3.379 and 3.436 Å, indicating that no coordination interaction is operative between the metal and these species. The corresponding calculated τ_4 value for the gas phase structure is 0.218, indicating, for the isolated complex, a structure closer to ideal square planar geometry.

The orbital diagram along with their energies and contributions from the ligands and metal, are given in figure 3S and table 5S. The energies of the highest singly occupied molecular orbital (SOMO) and lowest unoccupied molecular orbital (LUMO) for α -MOs are -6.84 and -2.53 eV, respectively. Whereas for β -MOs, the corresponding values are -6.85 and -3.67 eV, respectively. As a matter of fact, the SOMO–LUMO energy difference for α -MOs is larger ($\Delta E = 4.31$ eV) compared to the value of β -MOs ($\Delta E = 3.18$ eV). The

Table 4. Selected list of excitation energies of **1**.

| Excited state | Wavelength λ (nm) | Oscillatory strength (f) | Major contribution | Assignment [‡] |
|---------------|---------------------------|------------------------------|---|-------------------------|
| 1. | 828.87 | 0.0003 | SOMO-6(β) \rightarrow LUMO(β) (35%) | LMCT |
| 2. | 714.97 | 0.0008 | SOMO-4(β) \rightarrow LUMO(β) (31%) | LMCT |
| 3. | 583.69 | 0.0001 | SOMO-14(β) \rightarrow LUMO (β) (20%), SOMO-13(β) \rightarrow LUMO (β) (27%) | WMCT MMCT |
| 4. | 573.62 | 0.0016 | SOMO-18(β) \rightarrow LUMO(β) (34%) | MMCT |
| 5. | 462.14 | 0.0056 | SOMO(β) \rightarrow LUMO(β) (98%) | LMCT |
| 6. | 408.57 | 0.0028 | SOMO-1(β) \rightarrow LUMO(β) (87%) | LMCT |
| 7. | 404.09 | 0.0039 | SOMO-2(β) \rightarrow LUMO(β) (88%) | LMCT |
| 8. | 398.34 | 0.0104 | SOMO-3(β) \rightarrow LUMO(β) (77%) | LMCT |
| 10. | 376.39 | 0.0013 | SOMO-10(β) \rightarrow LUMO(β) (19%), SOMO-4(β) \rightarrow LUMO(β) (53%) | WMCT LMCT |
| 14. | 349.40 | 0.0007 | SOMO-5(β) \rightarrow LUMO(β) (82%) | LMCT |
| 18. | 325.35 | 0.0387 | SOMO-9(β) \rightarrow LUMO(β) (14%), SOMO-6(β) \rightarrow LUMO(β) (25%) | LMCT LMCT |
| 19. | 319.72 | 0.0045 | SOMO-3(α) \rightarrow LUMO(α) (19%), SOMO-3(β) \rightarrow LUMO+1(β) (54%) | ILCT ILCT |
| 20. | 315.50 | 0.0079 | SOMO-3(α) \rightarrow LUMO(α) (16%), SOMO-2(α) \rightarrow LUMO(α) (28%), SOMO-2(β) \rightarrow LUMO+1(β) (40%) | ILCT ILCT ILCT |
| 22. | 301.03 | 0.0059 | SOMO-1(α) \rightarrow LUMO(α) (45%), SOMO-1(β) \rightarrow LUMO+1(β) (45%) | ILCT ILCT |
| 23. | 297.21 | 0.0002 | SOMO-16(β) \rightarrow LUMO(β) (17%), SOMO-7(β) \rightarrow LUMO(β) (58%) | MMCT WMCT |
| 25. | 291.00 | 0.0013 | SOMO(α) \rightarrow LUMO+1(α) (25%), SOMO(β) \rightarrow LUMO+2(β) (62%) | ILCT ILCT ILCT |
| 30. | 270.02 | 0.0041 | SOMO-10(β) \rightarrow LUMO(β) (27%), SOMO-9(β) \rightarrow LUMO(β) (24%) | WMCT LMCT |
| 32. | 266.77 | 0.0003 | SOMO-2(α) \rightarrow LUMO+1(α) (53%), SOMO-2(β) \rightarrow LUMO+2(β) (19%) | ILCT ILCT |
| 34. | 259.45 | 0.007 | SOMO-1(α) \rightarrow LUMO+1(α) (42%), SOMO-1(β) \rightarrow LUMO+2(β) (52%) | ILCT ILCT |
| 35. | 257.63 | 0.013 | SOMO-4(β) \rightarrow LUMO+1(β) (36%) | ILCT |
| 37. | 253.56 | 0.0364 | SOMO-11(β) \rightarrow LUMO(β) (47%), SOMO-10(β) \rightarrow LUMO(β) (11%) | WMCT WMCT |
| 38. | 248.31 | 0.1792 | SOMO-5(α) \rightarrow LUMO(α) (15%), SOMO-5(β) \rightarrow LUMO+1(β) (30%) | ILCT ILCT |
| 40. | 243.53 | 0.1196 | SOMO-12(β) \rightarrow LUMO(β) (64%) | WMCT |
| 41. | 241.63 | 0.0041 | SOMO-13(β) \rightarrow LUMO(β) (33%) | MMCT |
| 51. | 223.59 | 0.1169 | SOMO-9(α) \rightarrow LUMO(α) (10%), SOMO-5(α) \rightarrow LUMO+1(α) (29%), SOMO-4(α) \rightarrow LUMO+1(α) (20%) | ILCT ILCT ILCT |
| 54. | 217.65 | 0.0009 | SOMO(α) \rightarrow LUMO+3(α) (38%), SOMO(β) \rightarrow LUMO+4(β) (41%) | ILCT LMCT |
| 55. | 213.94 | 0.0067 | SOMO-14(β) \rightarrow LUMO(β) (40%) | WMCT |
| 57. | 208.66 | 0.0028 | SOMO-10(α) \rightarrow LUMO(α) (46%), SOMO-9(α) \rightarrow LUMO(α) (10%), SOMO-10(β) \rightarrow LUMO+1(β) (14%) | WLCT WLCT WLCT |

[‡]M = metal; L = 2,5-pdc; W = water; MMCT = intra-metal charge transfer; LMCT = 2,5-pdc to metal charge transfer; WMCT = water to metal charge transfer; ILCT = intra-ligand charge transition in 2,5-pdc and WLCT = water to 2,5-pdc charge transfer.

SOMO and LUMO of α -MOs have a contribution from 2,5-pdc of 97 and 99%, respectively, while for β -MOs, SOMO has 98% contribution from 2,5-pdc and LUMO has 67% contribution from copper function. In summary, SOMO's of both α -MOs and β -MOs are largely characterized by the 2,5-pdc ligand orbitals ($\geq 97\%$), while LUMO of α -MOs has entirely 2,5-pdc orbital character (99%), but LUMO of β -MOs is characterized by copper orbitals (67%).

Table 5. Selected UV–vis energy transition at the TD-DFT/B3LYP level for **1** in methanol.

| Excited state | λ_{cal} (nm), ϵ_{cal} ($\text{M}^{-1}\text{cm}^{-1}$), (eV) | Oscillator strength (f) | λ_{exp} (nm), ϵ_{exp} ($\text{M}^{-1}\text{cm}^{-1}$), (eV) | Key transition | Character |
|-----------------|--|-----------------------------|--|---|----------------------|
| D ₅₁ | 223.59, 14675.67, (5.54) | 0.1189 | 226, 352, (5.48) | SOMO-9(α) \rightarrow LUMO(α) (10%), SOMO-5(α) \rightarrow LUMO+1(α) (29%), SOMO-4(α) \rightarrow LUMO+1(α) (20%) | ILCT ILCT ILCT |
| D ₃₂ | 266.77, 3593.12, (4.64) | 0.0009 | 266, 268, (4.66) | SOMO-2(α) \rightarrow LUMO+1(α) (53%), SOMO-2(β) \rightarrow LUMO+2(β) (19%) | ILCT ILCT |

Note: ILCT = intra-ligand charge transition in 2,5-pdc.

To gain detailed insight into the electronic transitions, TD-DFT calculation in methanol using CPCM was performed. The theoretically possible spin-allowed doublet-doublet electronic transitions with their assignments are listed in table 4. For **1A**, the TD-DFT results show that [SOMO-10(α) \rightarrow LUMO(α); SOMO-9(α) \rightarrow LUMO(α); SOMO-10(β) \rightarrow LUMO+1(β)] and [SOMO-6(β) \rightarrow LUMO(β)] are the possible highest and lowest energy electronic transitions, respectively. The highest energy electronic transitions for **1A** are ILCT (intra-ligand charge transfer in 2,5-pdc) and WLCT (water to 2,5-pdc charge transfer) in nature, and the lowest energy electronic transition is LMCT (2,5-pdc to metal charge transfer) in nature. In **1**, the experimental electronic transitions at 226 nm [SOMO-9(α) \rightarrow LUMO(α); SOMO-5(α) \rightarrow LUMO+1(α); SOMO-4(α) \rightarrow LUMO+1(α)] and 266 nm [SOMO-2(α) \rightarrow LUMO+1(α); SOMO-2(β) \rightarrow LUMO+2(β)] may be attributed to ILCT transitions (figure 1, table 5).

4. Conclusion

The crystal packing of Cu(pyridine-2,5-dicarboxylate) complex reported here shows a supramolecular 3-D architecture built by a cooperative H-bonding scheme involving coordinated and lattice water molecules as well as off-center anti-parallel π - π stacking interactions. The network is a rare example of a supramolecular system comprising $R_4^2(12)$ and $R_6^4(24)$ types of cyclic supramolecular synthons. DFT calculation on the isolated compound shows significant deviations with respect to the structure derived from the X-ray diffraction. TD-DFT calculation was performed and theoretically possible spin allowed doublet-doublet electronic transitions along with their assignments have been discussed.

Supplementary material

Tables showing experimental and theoretical IR spectral data, off-center anti-parallel π - π stacking interaction of py rings, C=O $\cdots\pi$ interaction data, H-bond parameters, MOs with their energies and compositions, and figures of fluorescence spectrum, optimized geometry in gas phase, and surface plot of some frontier molecular orbital. CCDC 957022 contains the supplementary crystallographic data for the copper complex. This data can be obtained free of charge via <http://www.ccdc.cam.ac.uk/conts/retrieving.html>, or from the Cambridge Crystallographic Data Center, 12 Union Road, Cambridge CB2 1EZ, UK; Fax: (044) 1223-336-033; or E-mail: deposit@ccdc.cam.ac.uk.

Acknowledgements

Dr Subal Chandra Manna acknowledges CSIR, Government of India [CSIR Project No. 01 (2743)/13/EMR-II] for financial support.

References

- [1] (a) L. Orola, M.V. Veidis, I. Mutikainen, I. Sarcevic. *Cryst. Growth Des.*, **11**, 4009 (2011); (b) X. Feng, H. Du, K. Chen, X. Xiao, S.-X. Luo, S.-F. Xue, Y.-Q. Zhang, Q.-J. Zhu, Z. Tao, X.-Y. Zhang, G. Wei. *Cryst. Growth Des.*, **10**, 2901 (2010); (c) S. Guha, M.G.B. Drew, A. Banerjee. *Cryst. Growth Des.*, **10**, 4716 (2010); (d) R. Robson, In *Comprehensive Supramolecular Chemistry*, J.L. Atwood, J.E.D. Davies, D.D. MacNicol, F. Vögtle, J.-M. Lehn (Eds), Vol. 6, pp. 733–755, Pergamon, Oxford (1997).
- [2] (a) A. Bacchi, M. Carcelli, P. Pelagatti, G. Rispoli, D. Rogolino. *Cryst. Growth Des.*, **12**, 387 (2012); (b) J.-H. Deng, D.-C. Zhong, X.-Z. Luo, H.-J. Liu, T.-B. Lu. *Cryst. Growth Des.*, **12**, 4861 (2012); (c) S. Khullar, S.K. Mandal. *Cryst. Growth Des.*, **12**, 5329 (2012); (d) B. Moulton, M.J. Zaworotko. *Chem. Rev.*, **101**, 1629 (2001).
- [3] (a) S. Subramanian, M.J. Zaworotko. *Angew. Chem. Int. Ed. Engl.*, **34**, 2127 (1995); (b) Y. Wan, H. Yang, D. Zhao. *Acc. Chem. Res.*, **39**, 423 (2006).
- [4] J. Zhang, K. Zhang, X. Huang, W. Cai, C. Zhou, S. Liu, F. Huang, Y. Cao. *J. Mater. Chem.*, **22**, 12759 (2012).
- [5] G.R. Desiraju. *J. Chem. Soc., Dalton Trans.*, 3745 (2000).
- [6] (a) G.R. Desiraju. *Crystal Engineering: The Design of Organic Solids*, Elsevier, Amsterdam (1989); (b) G.R. Desiraju, T. Steiner. *The Weak Hydrogen Bond in Structural Chemistry and Biology*, Oxford University Press, New York (1999).
- [7] (a) S.C. Manna, S. Mistri, A.D. Jana. *CrystEngComm*, **14**, 7415 (2012); (b) S.C. Manna, E. Zangrando, J. Ribas, N. Ray Chaudhuri. *Eur. J. Inorg. Chem.*, 1400 (2008).
- [8] (a) E. Tiekink, J. Zukerman-Schpector (Eds), *The Importance of Pi-Interactions in Crystal Engineering – Frontiers in Crystal Engineering*, Wiley, Singapore (2012); (b) C.R. Martinez, B.L. Iverson. *Chem. Sci.*, **3**, 2191 (2012); (c) A.K. Ghosh, A.D. Jana, D. Ghoshal, G. Mostafa, N. Ray Chaudhuri. *Cryst. Growth Des.*, **6**, 701 (2006); (d) Y.-Q. Sun, C.-K. Tsang, Z. Xu, G. Huang, J. He, X.-P. Zhou, M. Zeller, A.D. Hunter. *Cryst. Growth Des.*, **8**, 1468 (2008); (e) W. Niu, M.D. Smith, J.J. Lavigne. *Cryst. Growth Des.*, **6**, 1274 (2006).
- [9] (a) S. Grimme. *Angew. Chem. Int. Ed.*, **47**, 3430 (2008). (b) D.M. Rogers, J.D. Hirst, E. Lee, T. Wright. *Chem. Phys. Lett.*, **427**, 410 (2006); (c) S. Tsuzuki, K. Honda, T. Uchimaru, M. Mikami. *J. Chem. Phys.*, **122**, 144323–144328 (2005); (d) B.K. Mishra, N. Sathyamurthy. *J. Phys. Chem. A*, **109**, 6 (2005).
- [10] (a) S.C. Manna, S. Konar, E. Zangrando, K. Okamoto, J. Ribas, N. Ray Chaudhuri. *Eur. J. Inorg. Chem.*, 4646 (2005); (b) L. Tian, S.Y. Zhou. *J. Coord. Chem.*, **66**, 2863 (2013); (c) L. Zhao, F. Guo. *J. Coord. Chem.*, **66**, 2940 (2013); (d) S.-C. Chen, J. Qin, Z.-H. Zhang, M. Hu, F.-A. Sun, L. Liu, M.-Y. He, Q. Chen. *J. Coord. Chem.*, **66**, 1924 (2013); (e) J.-P. Zou, S.-C. Dai, W.-T. Guan, H.-B. Yang, Y.-F. Feng, X.-B. Luo. *J. Coord. Chem.*, **65**, 2877 (2012); (f) R. Gupta, S. Sanotra, H. Nawaz Sheikh, B. Kalsotra, V.K. Gupta, Rajnikant. *J. Coord. Chem.*, **65**, 3917 (2012); (g) S.C. Manna, E. Zangrando, N. Ray Chaudhuri. *J. Mol. Struct.*, **877**, 145 (2008).
- [11] (a) S.C. Manna, K. Okamoto, E. Zangrando, N. Ray Chaudhuri. *CrystEngComm*, **9**, 199 (2007); (b) S.C. Manna, E. Zangrando, J. Ribas, N. Ray Chaudhuri. *Dalton Trans.*, 1383 (2007); (c) S.C. Manna, E. Zangrando, J. Ribas, N. Ray Chaudhuri. *Eur. J. Inorg. Chem.*, 4592 (2007); (d) S. Konar, S.C. Manna, E. Zangrando, T. Mallah, J. Ribas, N. Ray Chaudhuri. *Eur. J. Inorg. Chem.*, 4202 (2004); (e) S.C. Manna, E. Zangrando, M.G.B. Drew, J. Ribas, N. Ray Chaudhuri. *Eur. J. Inorg. Chem.*, 481 (2006); (f) S.C. Manna, E. Zangrando, A. Bencini, C. Benelli, N. Ray Chaudhuri. *Inorg. Chem.*, **45**, 9114 (2006).
- [12] H. Eshtiagh-Hosseini, M. Mirzaei, M. Biabani, V. Lippolis, M. Chahkandi, C. Bazzicalupidi. *CrystEngComm*, **15**, 6752 (2013).
- [13] D.D. Perrin, W.L.F. Armarego, D.R. Perrin. *Purification of Laboratory Chemicals*, Pergamon Press, Oxford (1980).
- [14] Bruker. *Apex and Saint Programs*, Bruker AXS Inc., Madison, Wisconsin, USA (2007).
- [15] Bruker. *SADABS*, Bruker AXS Inc., Madison, Wisconsin, USA (2001).
- [16] G.M. Sheldrick. *Acta Cryst.*, **A64**, 112 (2008).
- [17] L.J. Farrugia. *J. Appl. Cryst.*, **45**, 849 (2012).
- [18] K. Brandenburg. *DIAMOND (Version 3.2i)*, Crystal Impact GbR, Bonn, Germany (1999).
- [19] M.J. Frisch, G.W. Trucks, H.B. Schlegel, G.E. Scuseria, M.A. Robb, J.R. Cheeseman, G. Scalmani, V. Barone, B. Mennucci, G.A. Petersson, H. Nakatsuji, M. Caricato, X. Li, H.P. Hratchian, A.F. Izmaylov, J. Bloino, G. Zheng, J.L. Sonnenberg, M. Hada, M. Ehara, K. Toyota, R. Fukuda, J. Hasegawa, M. Ishida, T. Nakajima, Y. Honda, O. Kitao, H. Nakai, T. Vreven, J.A. Montgomery Jr, J.E. Peralta, F. Ogliaro,

- M. Bearpark, J.J. Heyd, E. Brothers, K.N. Kudin, V.N. Staroverov, R. Kobayashi, J. Normand, K. Raghavachari, A. Rendell, J.C. Burant, S.S. Iyengar, J. Tomasi, M. Cossi, N. Rega, J.M. Millam, M. Klene, J.E. Knox, J.B. Cross, V. Bakken, C. Adamo, J. Jaramillo, R. Gomperts, R.E. Stratmann, O. Yazyev, A.J. Austin, R. Cammi, C. Pomelli, J.W. Ochterski, R.L. Martin, K. Morokuma, V.G. Zakrzewski, G.A. Voth, P. Salvador, J.J. Dannenberg, S. Dapprich, A.D. Daniels, O. Farkas, J.B. Foresman, J.V. Ortiz, J. Cioslowski, D.J. Fox. *Gaussian 09, Revision A.02*, Gaussian, Inc., Wallingford, CT (2009).
- [20] C. Lee, W. Yang, R.G. Parr. *Phys. Rev. B*, **37**, 785 (1988).
- [21] P.J. Hay, W.R. Wadt. *J. Chem. Phys.*, **82**, 270 (1985).
- [22] (a) R. Bauernschmitt, R. Ahlrichs. *Chem. Phys. Lett.*, **256**, 454 (1996); (b) R.E. Stratmann, G.E. Scuseria, M.J. Frisch. *J. Chem. Phys.*, **109**, 8218 (1998); (c) M.E. Casida, C. Jamorski, K.C. Casida, D.R. Salahub. *J. Chem. Phys.*, **108**, 4439 (1998).
- [23] (a) V. Barone, M. Cossi. *J. Phys. Chem. A*, **102**, 1995 (1998); (b) M. Cossi, V. Barone. *J. Chem. Phys.*, **115**, 4708 (2001); (c) M. Cossi, N. Rega, G. Scalmani, V. Barone. *J. Comput. Chem.*, **24**, 669 (2003).
- [24] N.M. O'Boyle, A.L. Tenderholt, K.M. Langner. *J. Comput. Chem.*, **29**, 839 (2008).
- [25] K. Nakamoto. *Infrared Spectra of Inorganic and Coordination Compounds*, Wiley, New York (1997).
- [26] M.C. Etter, J.C. MacDonald, J. Bernstein. *Acta Crystallogr.*, **B46**, 256 (1990).
- [27] E. Martin, S. Sanjay. *Acc. Chem. Res.*, **40**, 197 (2007).
- [28] H. Kumagai, H. Sobukawa, M. Kurmoo. *J. Mater. Sci.*, **43**, 2123 (2008).
- [29] D. Min, S.S. Yoon, D.-Y. Jung, C.Y. Lee, Y. Kim, W.S. Han, S.W. Lee. *Inorg. Chim. Acta*, **324**, 293 (2001).
- [30] S.M. Humphrey, T.J.P. Angliss, M. Aransay, D. Cave, L.A. Gerrard, G.F. Weldon, P.T. Wood. *Z. Anorg. Allg. Chem.*, **633**, 2342 (2007).
- [31] S.-T. Chuang, F.-M. Shen, T.-S. Kuo, K.-B. Shiu. *J. Chin. Chem. Soc.*, **54**, 893 (2007).
- [32] J.M. Andrić, G.V. Janjić, D.B. Ninković, S.D. Zarić. *Phys. Chem. Chem. Phys.*, **14**, 10896 (2012).
- [33] A.W. Addison, T.N. Rao, J. Reedijk, J.V. Rijn, G.C. Verschoor. *J. Chem. Soc., Dalton Trans.*, 1349 (1984).